Structures 76 (2025) 109052

Contents lists available at ScienceDirect

Structures

journal homepage: www.elsevier.com/locate/structures

Automatic response prediction in a digital twin framework for regional bridges group

Wenlong Zhao [a,b], Chunfeng Wan [a,b,*], Xiaonan Zhang [a], Guangcai Zhang [a], Youliang Ding [a], Liyu Xie [c], Haoyan Peng [a], Songtao Xue [c,d]

[a] Southeast University, Key Laboratory of concrete and prestressed concrete structure of Ministry of Education, Nanjing 210096, China
[b] Advanced Ocean Institute of Southeast University, Nantong 226000, China
[c] Department of Disaster Mitigation for Structures, Tongji University, Shanghai 200092, China
[d] Department of Architecture, Tohoku Institute of Technology, Sendai, Miyagi 982-8577, Japan

ARTICLE INFO

Keywords:
Bridge groups
Digital twin
Vehicle load effect
Deep learning
Structural health monitoring

ABSTRACT

Bridges are essential components of transportation infrastructure, real-time monitoring of their structural conditions can provide valuable information for maintenance strategies. By with advanced structural health monitoring systems, stakeholders can gain critical insights into the condition and safety of bridges, thereby optimizing maintenance efforts. However, it is unrealistic to expect that every bridge within a regional network will be equipped with extensive structural health monitoring and weigh-in-motion systems. This paper therefore presents a digital twin system for bridges group aimed at achieving the working condition perception for all bridges within the regional transportation network. In physical space, collecting vehicle information and structural response data from bridges. In the corresponding digital space, numerical models are established for each bridge of a regional bridge network, with traffic loads serving as the linking variable. The Transformer neural network is employed to facilitate safety warning across all bridges in the regional network. The analysis is conducted on predictions related to vehicle load responses and response between bridges, along with the effective integration of both measured and simulated data. The proposed digital twin system for bridges group is evaluated using three concrete bridges located in Jiangsu, China, indicating the feasibility of the prediction models and providing critical support for the advancement of intelligent transportation infrastructure systems.

1. Introduction

The advent of the Internet of things, big data, and cyber-physical systems has catalyzed the increasing importance of the concept of digitizing the physical world, with the "digital twin" (DT) serving as a notable illustration [1]. Now, the concept of the DT has developed into a more comprehensive notion, denoting a dynamic model that persistently updates and adapts in response to alterations in its physical counterpart [2,3]. Although it may easily resemble a traditional digital model, the fundamental distinction lies in the DT's dynamic linkage to its physical counterpart, enabling continuous data exchange. DT is acknowledged as a crucial technology within the framework of industry 4.0, driving innovations in smart manufacturing [4,5]. For example, DT can significantly enhance product design, manufacturing processes, and service delivery [6]. By simulating, evaluating, and optimizing production plans in a virtual environment, while simultaneously comparing real-time data from the physical domain with digital plans, DTs enable more precise and efficient manufacturing management [7]. As noted by Broo and Schooling [8], the principal advantage of DTs lies in their ability to integrate diverse datasets, allowing industries to design, construct, and operate infrastructure assets more rapidly, efficiently, and sustainably.

The utilization of DT in civil engineering remains in the early stages, particularly when compared to its application in the manufacturing and aerospace industries [9,10]. Structural health monitoring (SHM) systems, which gather data from sensors installed on structures, play a crucial role in assessing structural integrity and identifying associated safety risks [11–13]. These systems not only enhance the interaction between the physical structure and its digital counterpart but also facilitate a range of interactive functions. As a result, SHM is regarded as an especially promising domain for advancing DT technology in civil engineering. Informed decisions regarding the operation and maintenance of bridges are driven by the extensive sensor data and real-time

* Corresponding author at: Southeast University, Key Laboratory of concrete and prestressed concrete structure of Ministry of Education, Nanjing 210096, China.
E-mail address: wan@seu.edu.cn (C. Wan).

https://doi.org/10.1016/j.istruc.2025.109052
Received 18 November 2024; Received in revised form 11 March 2025; Accepted 25 April 2025
Available online 29 April 2025

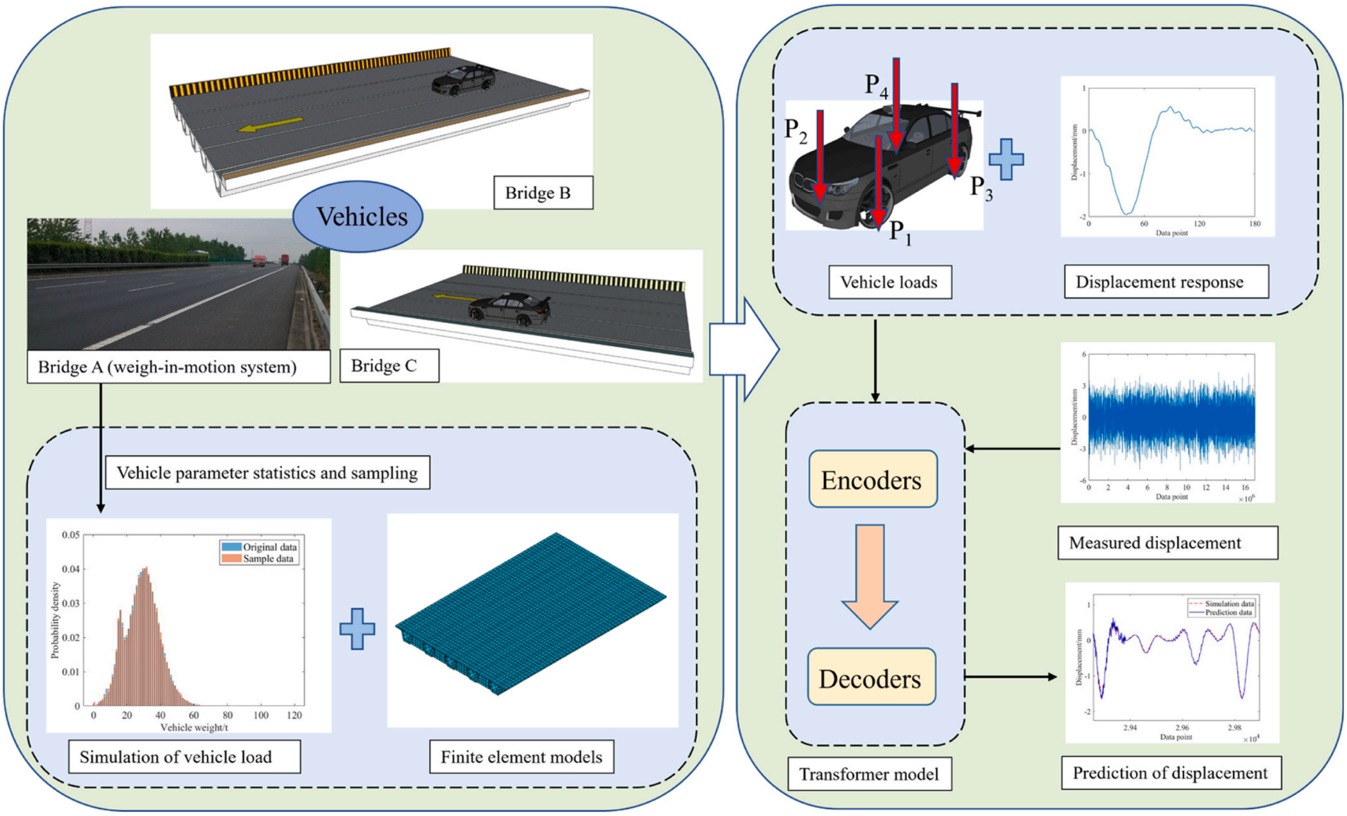

Fig. 1. Response prediction framework for regional bridge groups based on digital twin and deep learning.

evaluations produced by the virtual twin, which replicates the physical structure. These actions include security alerts [14], maintenance [15,16], and asset management [17,18], damage identification[19–21]. Ye et al. [22] developed a digital twin system specifically for bridge health monitoring, which integrated data-driven and model-based methodologies to optimize data processing and interpretation. Jiang et al. [23,24] utilized DT to forecast the fatigue life of steel bridges, allowing for real-time interaction between physical and virtual models. Kang et al. [25] introduced a multimedia knowledge-based technique that incorporates digital twins for bridge health monitoring. Their methodology involved using sensor data to update digital simulation models, followed by the simulation of extreme scenarios to ensure the safety of the bridge. Dang et al. [26] proposed a digital twin framework for SHM, which achieved a damage detection accuracy of 92 %. Additionally, Zhao et al. [27] employed long-term monitoring data to update transverse distribution factors and influence lines, thus enabling real-time performance predictions.

Presently, bridge health monitoring systems predominantly focus on the collection and analysis of data derived directly from the bridge structure [28–32]. Consequently, the interactions between the model and its physical counterpart are primarily concentrated on the observed structural responses. Traffic load constitutes the primary live load that bridges encounter. When traffic load data is available, the computation of the corresponding structural responses using a digital model is well-established, characterized by low complexity and high efficiency. Therefore, measured traffic loads can function as a conduit for information exchange between the physical bridge and its digital twin, constituting an effective strategy for the implementation of digital twins in bridge systems.

With the widespread adoption of artificial intelligence technologies, increasingly sophisticated computer vision techniques have attracted the attention of researchers in the field of bridge health monitoring [33–35]. These techniques have also played a significant role in facilitating the use of traffic loads as an information exchange medium between the physical bridge and its digital twin. Xue et al. [36] established a digital twin system that incorporates image recognition, target tracking, and data fusion technologies to facilitate the real-time identification of vehicle load positions on bridge decks. To establish a connection between traffic loads and bridge responses, Hou et al. [37] proposed a cyber-physical system framework for a highway corridor. This framework activates SHM systems to record responses and automatically correlates these responses with truck weights recorded by weigh-in-motion (WIM) systems, thereby illustrating the potential of employing measured traffic loads for DT applications. Additionally, Dan et al. [14] developed mechanical analysis models within the digital domain, utilizing measured traffic loads as the linking variable to facilitate condition monitoring and safety alerts for all bridges within a regional transport network. Furthermore, Yu et al. [38] investigated stress responses by integrating vehicle loads and temperature influences on fatigue damage states, subsequently updating the digital twin model with data obtained from WIM and SHM systems. Tang et al. [39] presented a cost-effective method for identifying vehicle loads on bridges by integrating video data with physical modeling. Reconstructed traffic flow was utilized on finite element modeling to predict the structural response induced by vehicle loads. However, the above research still has the following problems, which limit the application of this technology: (1) In the aspect of vehicle identification, there is a lack of research on vehicle identification technology in bad weather conditions such as rain and fog. (2) they were also limited by the need to collocate the WIM station and camera at the bridge.

Despite recent advancements, most existing research remains focused on individual bridges, often overlooking the interconnections within regional bridge networks and failing to fully exploit the available data. Moreover, the deployment of comprehensive structural health monitoring and weigh-in-motion systems remains limited to a small number of bridges, while many conventional structures still rely on

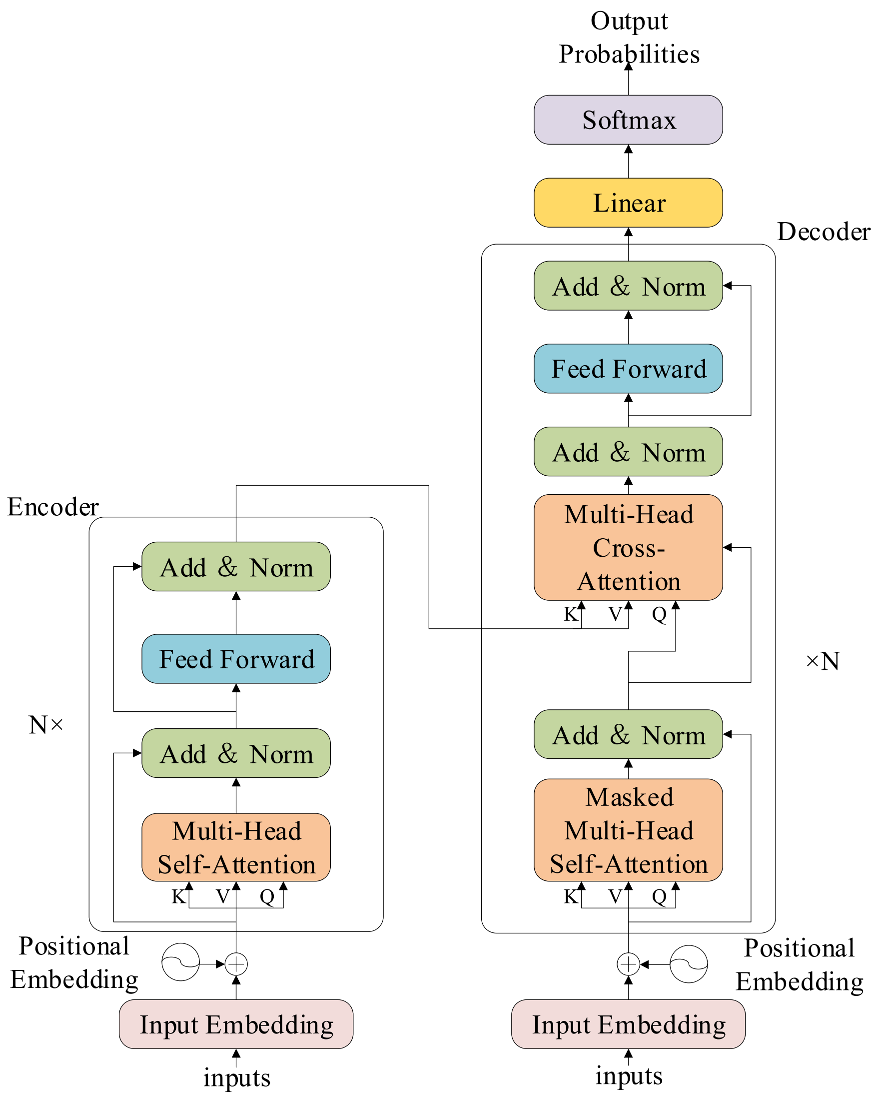

Fig. 2. Architecture of the Transformer.

periodic inspections, lacking real-time monitoring to inform intelligent operation and maintenance. Addressing these limitations, this paper studies the dynamic response behavior of a small bridge network, where only one bridge is equipped with SHM and WIM systems while others are not. Vehicle loads are utilized as the connecting variable to predict responses for bridges without SHM systems. Neural networks are employed to develop a digital twin-based response prediction model for the regional bridge network. This approach aims to compensate for the scarcity of monitoring equipment by efficiently utilizing vehicle load and structural response data. The paper studies both vehicle load response predictions and cross-bridge response predictions, integrating simulated and measured data to enhance the performance of the models, and validating the accuracy of the pre-trained response prediction models with actual vehicle responses. Finally, a comparative analysis with several machine learning methods is conducted, verifying the superiority of the adopted algorithm and the effectiveness of the method. The proposed digital twin system could significantly enhance the intelligent management and maintenance of regional bridge networks, contributing to more effective infrastructure operations.

2. Methodology

2.1. Digital twin model framework

Generally, the digital twin represents a dynamic model that continuously updates and adjusts based on changes in its physical counterpart. For the digital twin system of bridges, it integrates models, physical entities, and long-term monitoring data to facilitate interactions, achieving outcomes such as performance prediction, damage identification, and extreme scenario simulation. Therefore, this paper proposed the response prediction framework for regional bridge groups based on digital twin and deep learning to achieve regional intelligent management in Fig. 1. First, vehicle load data is collected using the weigh-in-motion system installed on one bridge. After classifying the vehicles, the velocity and weight of each vehicle type are fitted using the Gaussian distribution. Then, the Monte Carlo sampling method is employed to generate vehicle load information. Next, the finite element analysis is conducted for the bridges in the regional network. Data augmentation techniques are utilized to balance computational efficiency and data volume. Ultimately, Transformer-based prediction models are developed to estimate vehicle load-induced responses, with actual response data integrated to enhance the model's predictive accuracy.

Within the digital twin framework, vehicle loads are a key factor that connects the physical and digital space. The vehicle load responses for

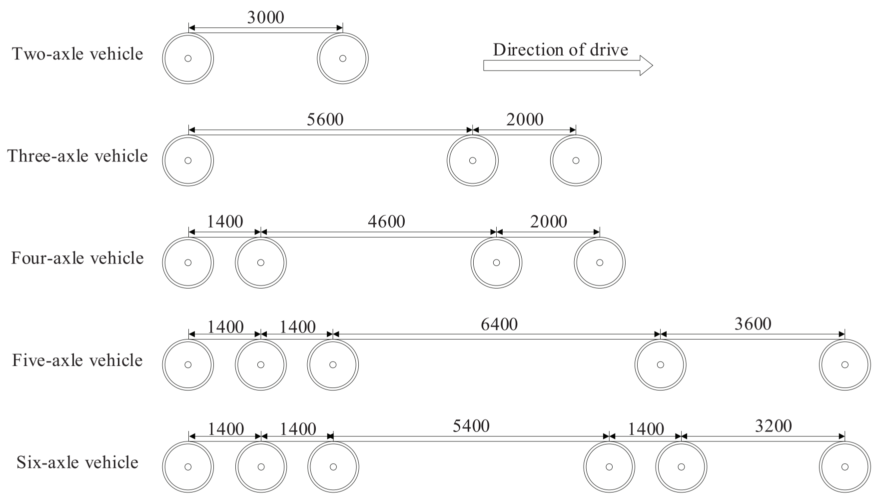

Fig. 3. Vehicle model.

Table 1
Axle weight ratio of each vehicle type.

Vehicle type	axle 1	axle 2	axle 3	axle 4	axle 5	axle 6
Two-axle vehicle	0.42	0.58	/	/	/	/
Three-axle vehicle	0.25	0.24	0.51	/	/	/
Four-axle vehicle	0.20	0.25	0.27	0.28	/	/
Five-axle vehicle	0.18	0.27	0.19	0.18	0.18	/
Six-axle vehicle	0.14	0.14	0.18	0.18	0.18	0.18

each bridge within the bridges group can be computed rapidly and efficiently using the pre-trained model, overcoming the barriers to response computations between bridges and enabling the intelligent management and maintenance of the entire bridge network.

2.2. Gaussian distribution and K-S test

The Gaussian mixture model (GMM) uses a linear combination of several normal distribution functions to approximate any probability density function, enabling the description of the joint probability distribution of random variables that are neither independent nor normally distributed. It is widely applied in engineering research fields, including network security[40], highway traffic flow prediction[41], and equipment operational status[42].

In real traffic conditions, the flow of road traffic is formed by the mixed movement of various types of vehicles. The velocity of the same type of vehicle can be fitted using multiple Gaussian distributions, particularly when categorized by the number of axles. Therefore, the velocity of a certain type of vehicle can be effectively represented by a Gaussian mixture model as follows:

$$\mathrm{p}\left\{v_k \middle| \left(\omega_\mathrm{i}, \mu_i, \sigma_i^2\right)\right\} = \sum_{i=1}^{n} \omega_\mathrm{i} g\left(v_k \middle| \mu_i, \sigma_i^2\right) \tag{1}$$

where v_k is the velocity of the k-th vehicle within a certain sampling interval ; n represents the number of Gaussian components in the GMM model, ω_i is the weight of the i-th Gaussian distribution and $\sum_{i=1}^{n} \omega_\mathrm{i} = 1$; $g\left(v_k \middle| \mu_i, \sigma_i^2\right)$ is the probability density function of the i-th type of Gaussian distribution is given by:

$$g\left(v_k \middle| \mu_i, \sigma_i^2\right) = \frac{1}{\sqrt{2\pi}\sigma_i} \exp\left[-\frac{1}{2\sigma_i^2}(v_k - \mu_i)^2\right] \tag{2}$$

where μ_i is the mean of the i-th type of Gaussian distribution; σ_i is the standard deviation of the i-th type of Gaussian distribution.

It should be emphasized that the GMM fundamentally assumes independent linear combinations. This inherent property limits its capacity to model dynamic interdependencies inherent in traffic flow phenomena, such as vehicle platooning effects and congestion-induced

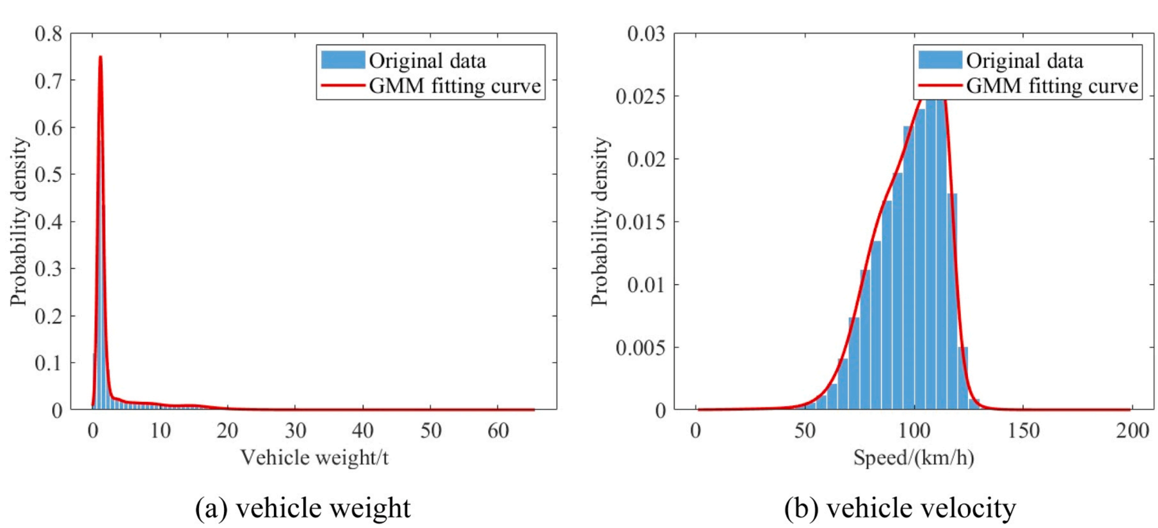

Fig. 4. Fitting curve of two-axle vehicles.

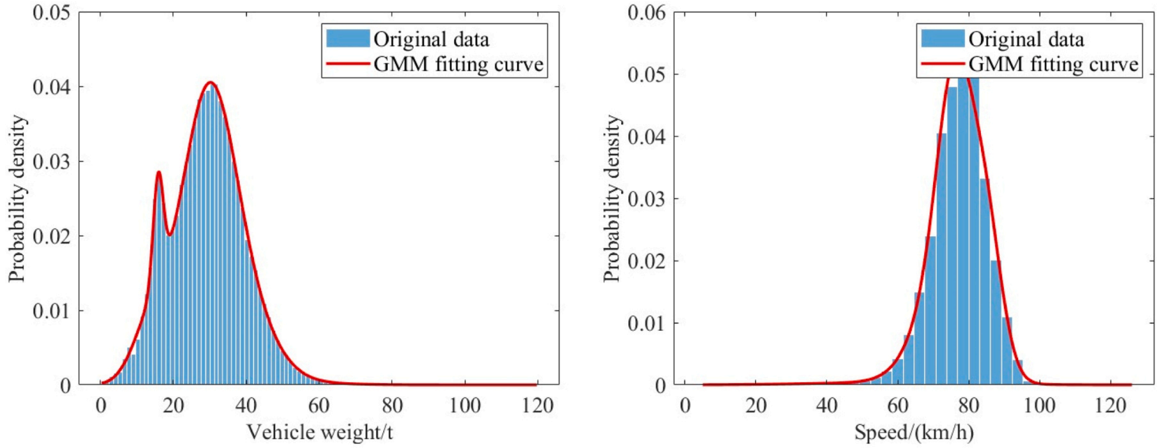

(a) vehicle weight (b) vehicle velocity

Fig. 5. Fitting curve of five-axle vehicles.

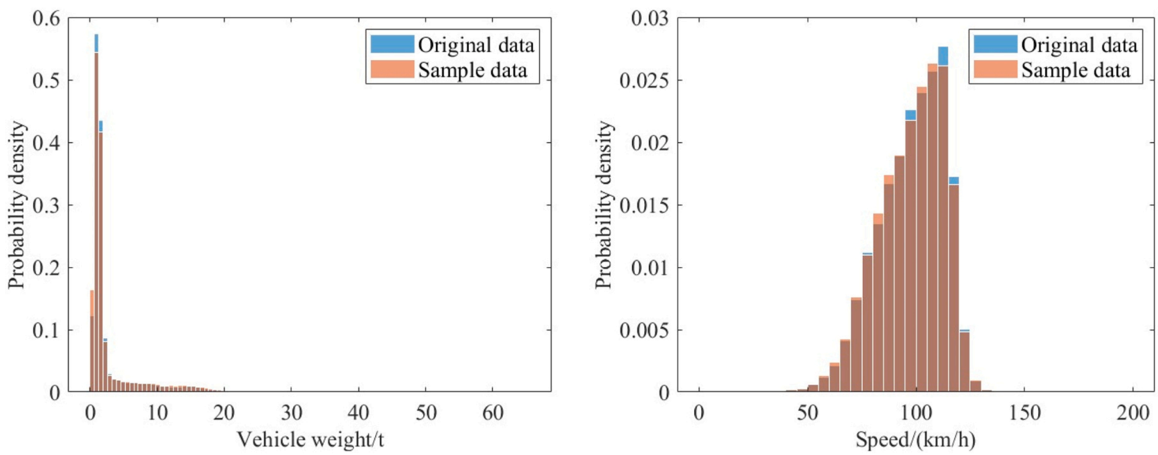

(a) vehicle weight (b) vehicle velocity

Fig. 6. Sample comparison of two-axle vehicles.

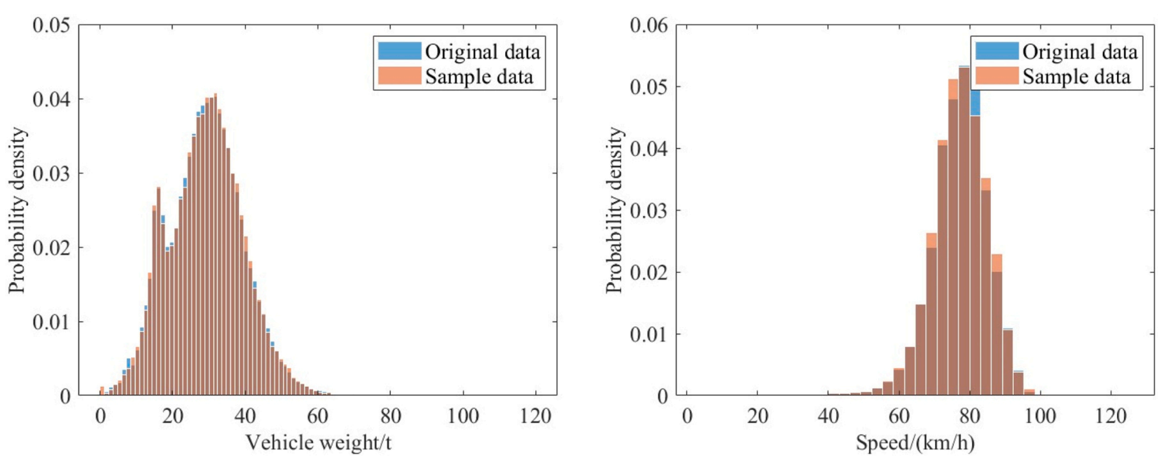

(a) vehicle weight (b) vehicle velocity

Fig. 7. Sample comparison of five-axle vehicles.

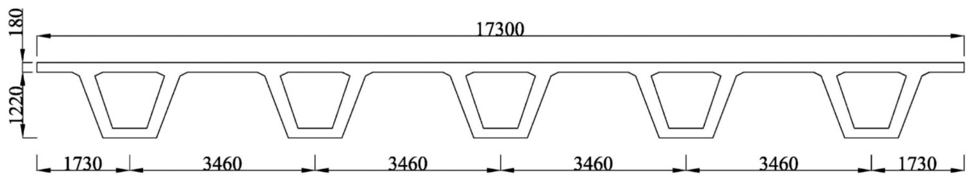

Fig. 8. Cross-section of bridge A.

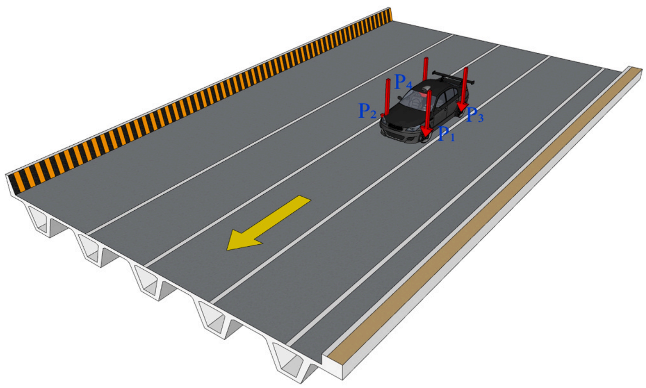

Fig. 9. The finite element model for bridge B.

Table 2
Loading cases.

Parameters of vehicle load	Case 1	Case 2	Case 3	Case 4	Case 5
Number of axles	2	3	4	5	6
Lane	Overtaking lane	Middle lane	Slow lane	Overtaking lane	Middle lane
Vehicle velocity (km/h)	113.74	71.95	63.90	74.47	64.08
Vehicle weight (t)	2.11	19.99	29.24	38.58	56.58
Axle 1 wt (t)	0.88	5.01	5.85	6.94	7.93
Axle 2 wt (t)	1.23	4.79	7.31	10.42	7.93
Axle 3 wt (t)	0	10.19	7.90	7.34	10.18
Axle 4 wt (t)	0	0	8.18	6.94	10.18
Axle 5 wt (t)	0	0	0	6.94	10.18
Axle 6 wt (t)	0	0	0	0	10.18
Vehicle length (m)	3	7.6	8	12.8	12.8
Wheelbase l_{12} (m)	3	2	2	3.6	3.2
Wheelbase l_{23} (m)	0	5.6	4.6	6.4	1.4
Wheelbase l_{34} (m)	0	0	1.4	1.4	5.4
Wheelbase l_{45} (m)	0	0	0	1.4	1.4
Wheelbase l_{56} (m)	0	0	0	0	1.4

load correlations. To address this theoretical constraint while maintaining computational tractability, a simplified vehicular loading protocol is adopted in simulation, where vehicles traverse the bridge sequentially, with each vehicle's load contribution being statistically independent. This strategic simplification serves two critical purposes: (1) it circumvents the computational complexities associated with modeling large-scale traffic interactions, and (2) it enables systematic quantification of individual vehicle-induced structural responses, thereby establishing a foundational understanding for future extensions to multi-vehicle loading scenarios.

The fitting effect is evaluated using the K-S test, also known as the Kolmogorov-Smirnov test. This method does not assess the deviation between the empirical distribution function $Fn(x_i)$ derived from subsamples and the fitted theoretical distribution $F(x_i)$ by intervals. Instead, the deviation between $Fn(x_i)$ and $F(x_i)$ is examined at each point. Consequently, the K-S test is relatively precise.

The K-S test statistic is

$$D = \underset{x}{MAX}|Fn(x_i) - F(x_i)| \tag{3}$$

where D represents the absolute maximum difference between the empirical distribution $Fn(x_i)$ and the theoretical distribution $F(x_i)$ for all samples x_i.

According to the K-S test theory, when $D<D$crit (where Dcrit is the critical value for the level of significance α), the samples x_i has no major difference between distributions $Fn(x_i)$ and $F(x_i)$ at the significance level α. Conversely, if $D\geq D$crit, there is a great difference at the 1−α confidence level. From (2−3), it is evident that a larger D value indicates a greater difference between the empirical distribution function $Fn(x_i)$ and the fitted theoretical distribution $F(x_i)$, suggesting a stronger ability to distinguish between the two distributions.

2.3. Transformer model

Before the introduction of the Transformer, Recurrent Neural Networks, particularly Long Short Term Memory (LSTM) [43] and Gated Recurrent Unit (GRU) [44], were extensively employed for sequence modeling and inference tasks, particularly machine translation. Transformer is a multilayer structure constructed by stacking Transformer blocks, as depicted in Fig. 2. The Transformer is characterized by a new novel positional encoding mechanism to capture time series information within the input data [45], and a multi-head self-attention mechanism to learn different linear transformations.

To fully use the position information of the sequence, relative position tokens are injected into the sequence. In this paper, we use sine and cosine functions of different frequencies:

$$PE_{(pos,2i)} = \sin\left(pos/10000^{2i/d_{model}}\right) \tag{4}$$

$$PE_{(pos,2i+1)} = \cos\left(pos/10000^{2i/d_{model}}\right) \tag{5}$$

where pos is the position, i is the dimension, and $d_{model} = 512$.

The input vector is represented as $X = [x_1, x_2, \ldots, x_n]$. To match a weight with the input vector, the equation is as follows:

$$Attention(Q, K, V) = Softmax\left(\frac{QK^T}{\sqrt{d_k}}\right)V \tag{6}$$

where Q, K, and V denote "query", "key", and "value", respectively; d_k is the scaling factor. For larger values of d_k, the dot products become too large, leading the Softmax function to operate in regions with very small gradients. To address this issue, the dot product is scaled by $\frac{1}{\sqrt{d_k}}$.

After obtaining the Attention output, it is sent to the subsequent component of the encoder, i.e., feedforward neural network. This network is fully connected and comprises two layers: the first layer utilizes a $ReLU$ activation function, while the second layer employs a linear activation function. The process can be expressed as follows:

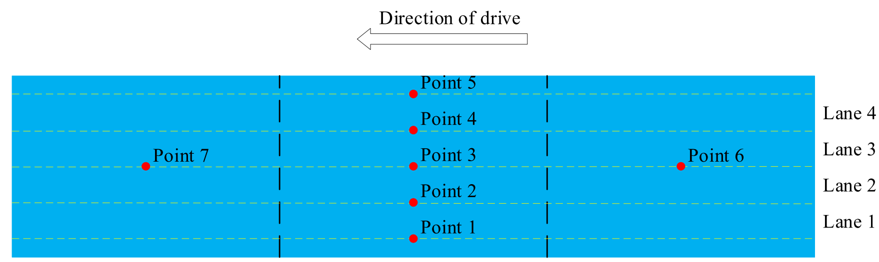

(a) Bridge A

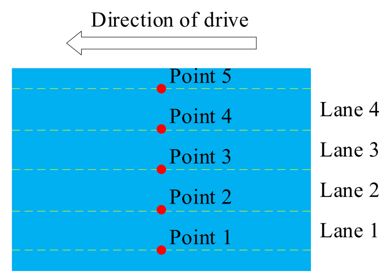

(b) Bridge B and C

Fig. 10. Layout of measurement points.

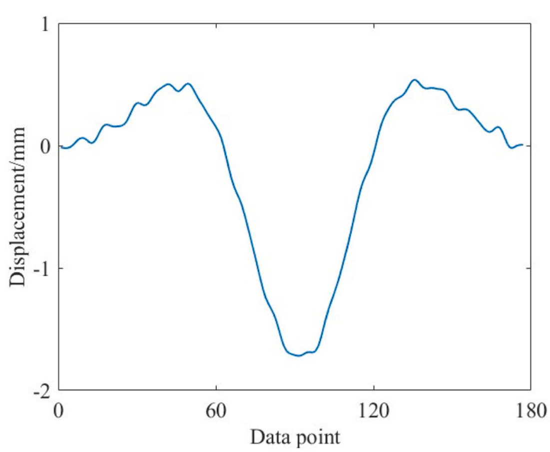

(a) measure point 3 of bridge A

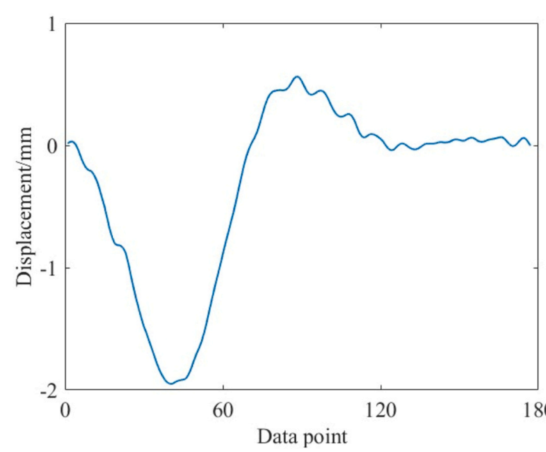

(b) measure point 6 of bridge A

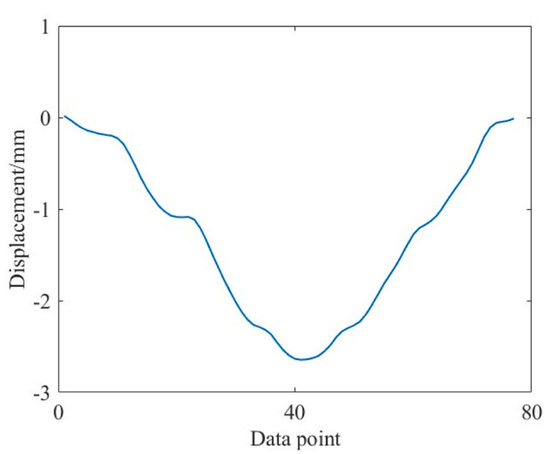

(c) measure point 3 of bridge B

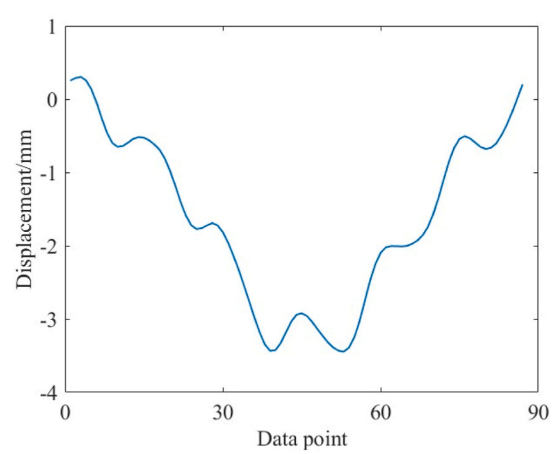

(d) measure point 3 of bridge C

Fig. 11. Displacement response of three bridges.

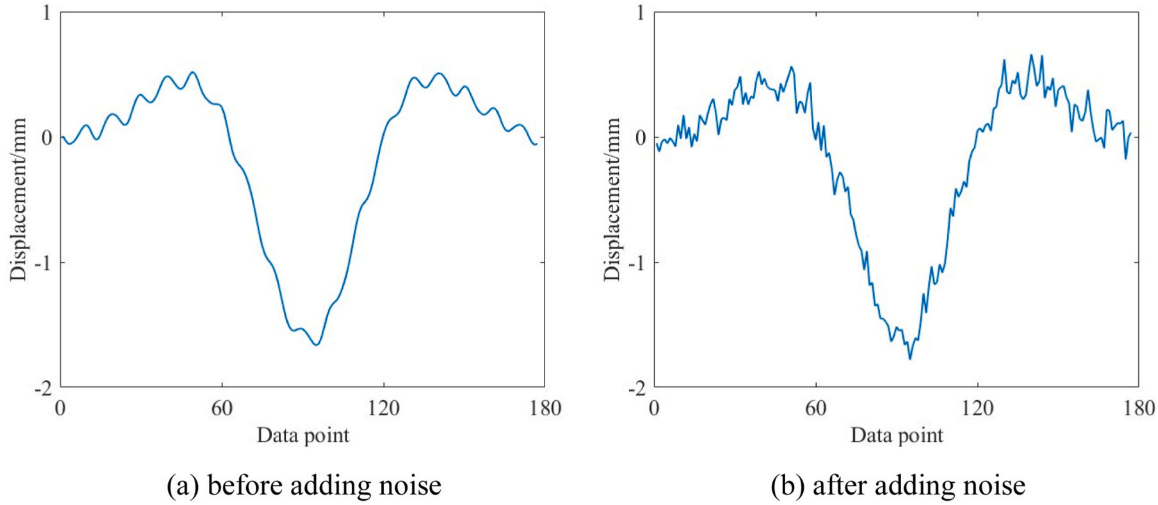

Fig. 12. Comparison before and after adding noise.

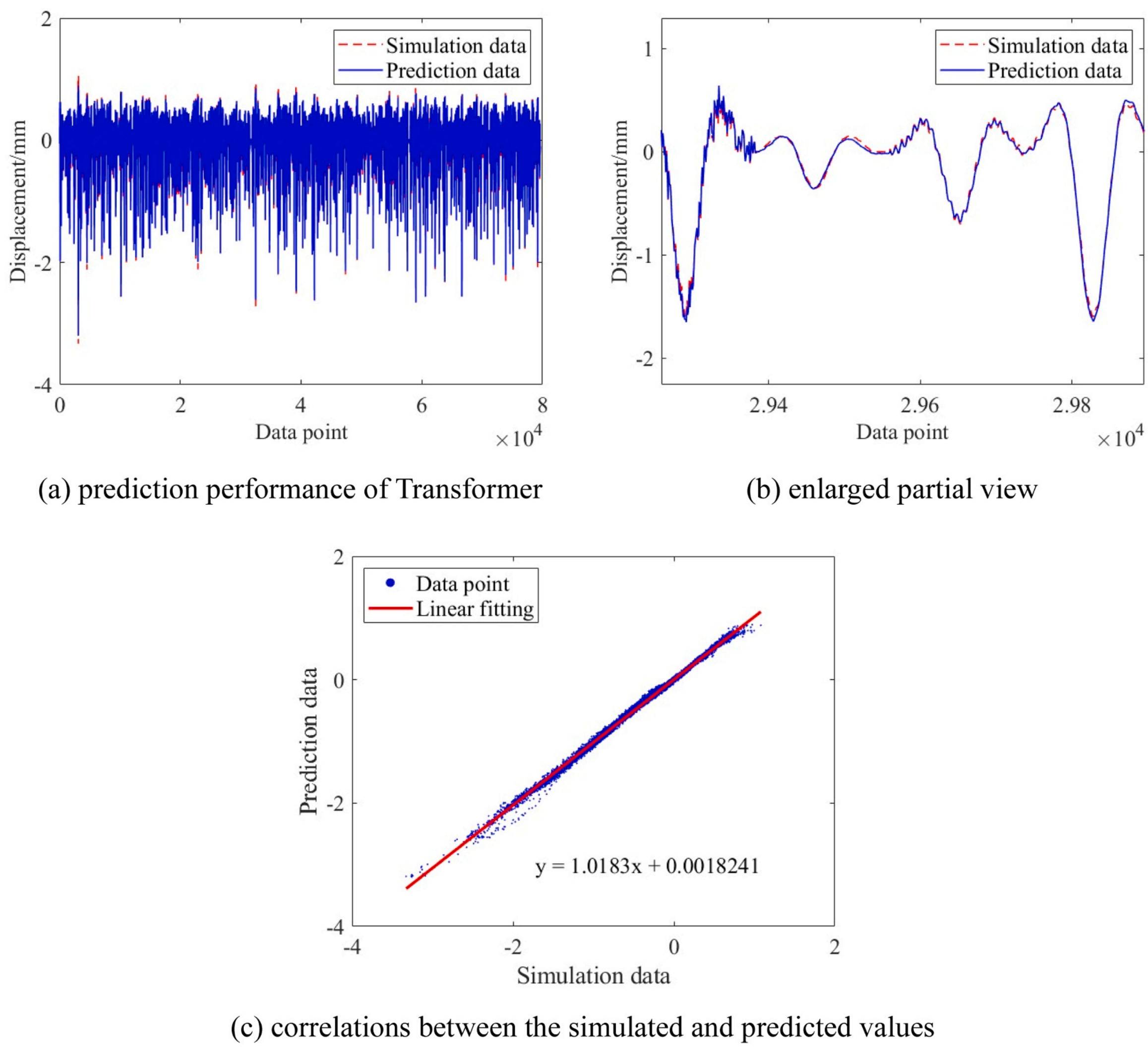

Fig. 13. Prediction results of measurement point 3 of bridge A.

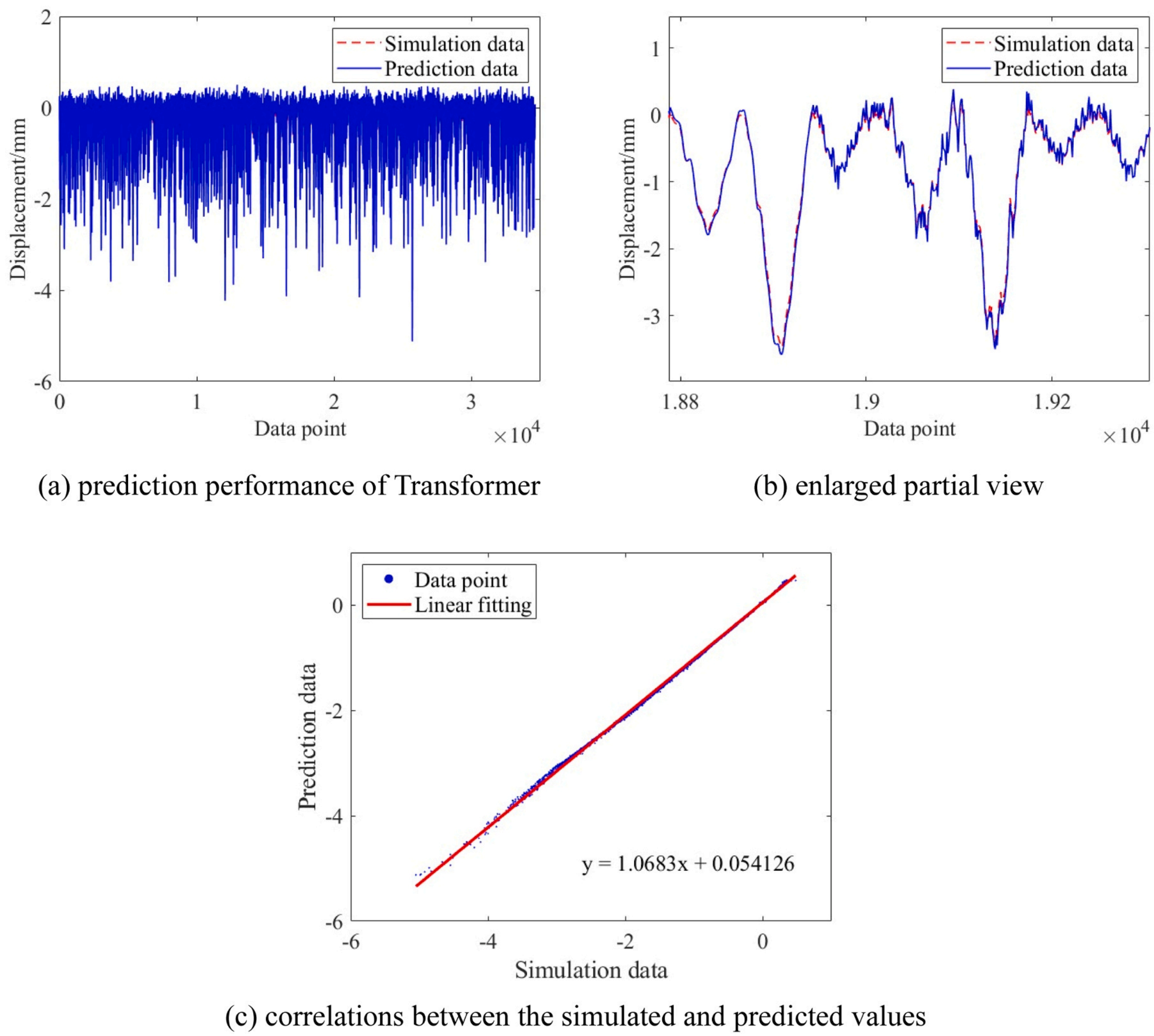

Fig. 14. Prediction results of measurement point 3 of bridge B.

Table 3
The evaluation of the prediction results for the three bridges using the Transformer model.

Bridge	T_a	$RMAE$	R^2
Medium span of bridge A	0.0056	0.2795	0.9970
Side span of bridge A	0.0011	0.0287	0.9999
Bridge B	0.0093	0.0702	0.9996
Bridge C	0.0051	0.0380	0.9996

$$FFN(x) = \max(0, xW_1 + b_1)W_2 + b_2 \tag{7}$$

Furthermore, multi-head attention allows the model to jointly attend to information from different representation subspaces at different positions.

$$MultiHead(Q, K, V) = Concat(head_1, head_2, \ldots, head_h)W^O \tag{8}$$

$$head_i = Attention\left(QW_i^Q, KW_i^K, VW_i^V\right) \tag{9}$$

In this paper,$Q, K, V \in R^{512}$,$h = 8$, $W^O \in R^{512\times512}$,$head_i \in R^{64}$,W_i^Q, W_i^K, $W_i^V \in R^{512\times64}$.

The Transformer model, which effectively and efficiently gains useful information of the sequences, addresses several limitations associated with traditional recurrent structures, including (1) the challenge of parallel feature extraction, (2) the difficulty in modeling long-range dependencies, (3) the key of gradient explosion and gradient vanishes. Although LSTM and GRU mitigate these problems to some extent, they do not completely resolve the weight accumulation resulting from multiple recurrences. Additionally, multiple self-attention layers can be stacked to construct a deep neural network, enabling Transformer to process millions or even billions of training samples.

Generally, Transformers are divided into three distinct categories: (1) encoder-only (e.g., for classification), (2) decoder-only (e.g., for language modeling), and (3) encoder–decoder (e.g., for machine translation).[46] Since the prediction of bridge response is a sequence-to-sequence (Seq2Seq) problem, the method proposed in this paper employs an encoder-decoder structure. This approach enables precise multi-input and multi-output regression modeling, thereby effectively capturing the spatiotemporal dynamic correlations present in multi-sensor data collected from SHM systems.

The loss function adopt here is the root mean square error (RMSE), Eq. (4).

$$RMSE = \sqrt{\frac{1}{n}\sum_{i=1}^{n}\left(\hat{y}_i - y_i\right)^2} \tag{10}$$

where $\hat{y}_i$ and y_i are the predicted value and the real value, respectively.

In this paper, the training employs the Adam optimizer with an initial learning rate of 0.001, a batch size of 50, and N = 3. The configurations of the computational platform are a 12th Gen Intel Core i5–12400F processor, and an NVIDIA GeForce RTX 2060 GPU. To better

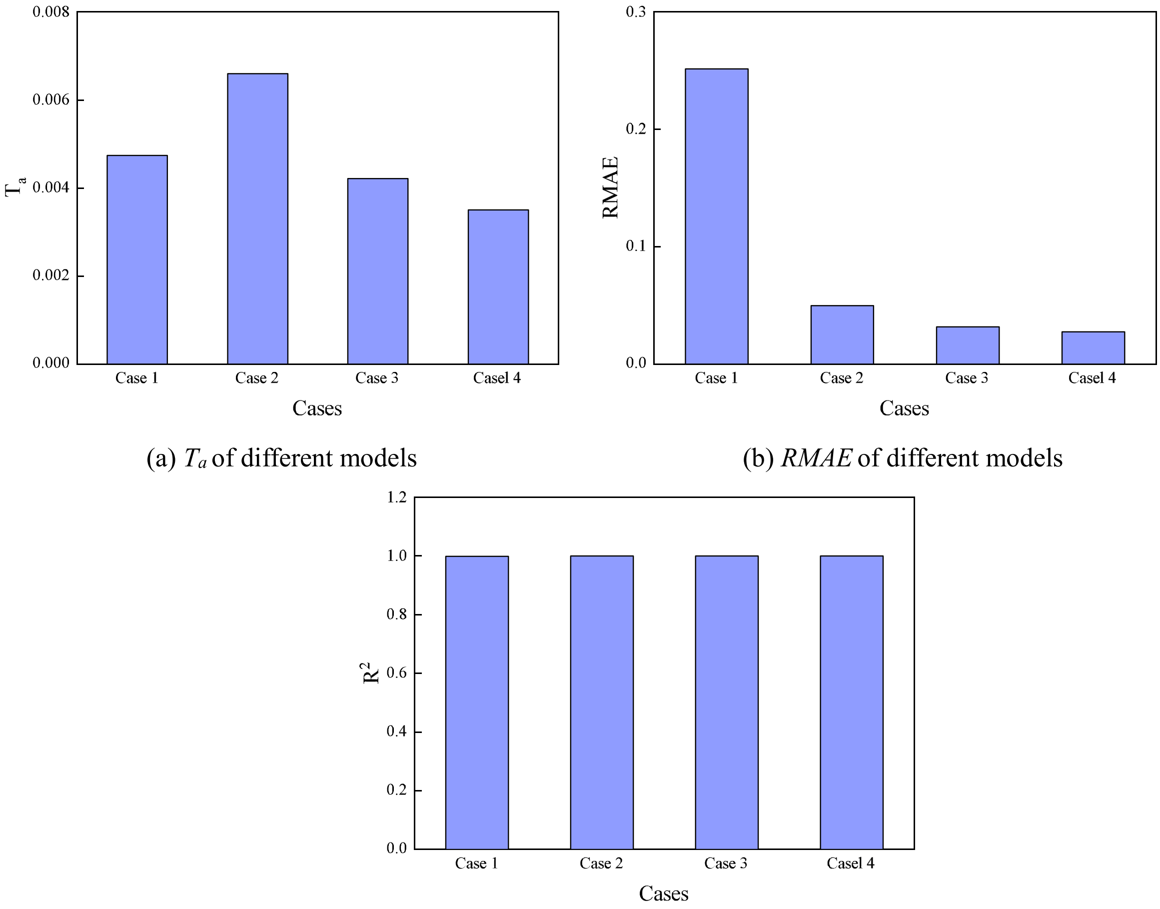

(a) T_a of different models

(b) *RMAE* of different models

(c) R^2 of different models

Fig. 15. The predictive performance of the four models.

evaluate the performance of the neural network model, T_a, relative mean absolute error (*RMAE*) and the coefficient of determination R^2 are used as evaluation metrics in this study. The calculation formula for T_a is provided as follows:

$$T_{\mathrm{a}} = \frac{\sqrt{\frac{1}{n}\sum_{i=1}^{n}(\widehat{y}_i - y_i)^2}}{A_t} \tag{11}$$

where A_t represents the difference between the maximum and minimum values of the target sequence data. A lower T_a indicates that the model prediction error is lower when the target data amplitude is the same, or that the target data amplitude is larger when the model prediction error is the same, both representing superior model prediction performance. Conversely, a higher T_a value suggests poorer model prediction performance.

The calculation for *RMAE* is defined as follows:

$$RMAE = \frac{\sum_{i=1}^{n}(\widehat{y}_i - y_i)^2}{\sum_{i=1}^{n} y_i} \tag{12}$$

The formula for calculating the coefficient of determination R^2 can be expressed as below:

$$R^2 = 1 - \frac{\sum_{i=1}^{n}(y_i - \widehat{y}_i)^2}{\sum_{i=1}^{n}(y_i - \overline{y})^2} \tag{13}$$

where $\overline{y}$ is the mean of the real value. The R^2 ranges from 0 to 1, where the value closer to 1 indicates a better fit of the model.

3. Numerical validation

To verify the proposed digital twin framework, numerical simulation is conducted at first. A regional bridge group which contains three primary bridges named Bridge A, Bridge B, and Bridge C, is used for analysis. Bridge A is equipped with a comprehensive health monitoring and weigh-in-motion systems, while bridges B and C, which are also concrete beam bridges, lack such systems. In this section, the vehicle data collected from the weigh-in-motion system of bridge A is first analyzed and categorized into distinct vehicle types. Vehicle weight and velocity are then fitted and simulated to generate traffic loads that conform to actual statistical distributions, which are subsequently applied to the finite element models of the three bridges in a regional network to obtain corresponding structural responses. To balance computational efficiency with data volume, 1500 datasets were initially generated through simulated loading. The dataset was further expanded to 4500 groups by augmenting the data with noise. Ultimately, the load-response prediction models were subsequently developed for all three bridges, followed by an analysis of four cases involving cross-bridge response prediction. Evaluation metrics confirm that each model demonstrates satisfactory predictive accuracy.

(a) bridge A

(b) substructure of bridge A

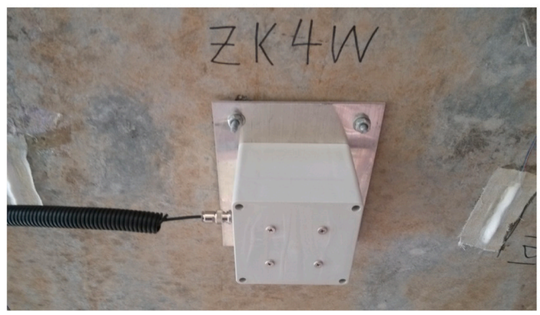

(c) dynamic displacement sensor

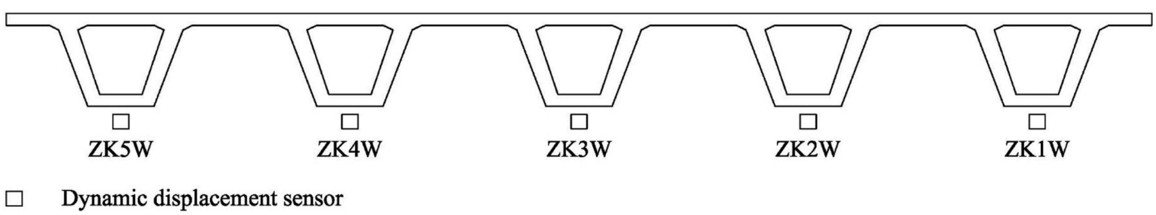

(d) sensor deployment of the midspan cross section

Fig. 16. Bridge A and sensor deployment.

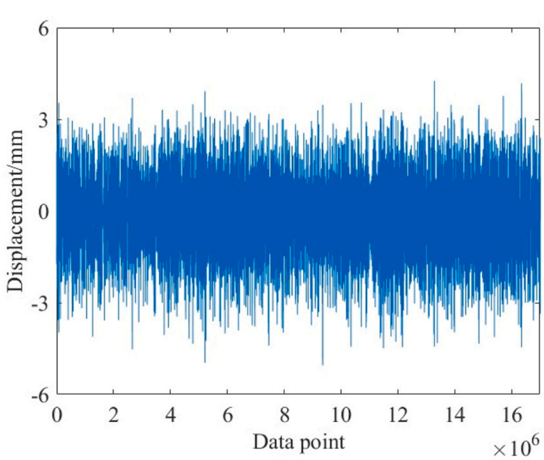

(a) measured displacement of bridge A

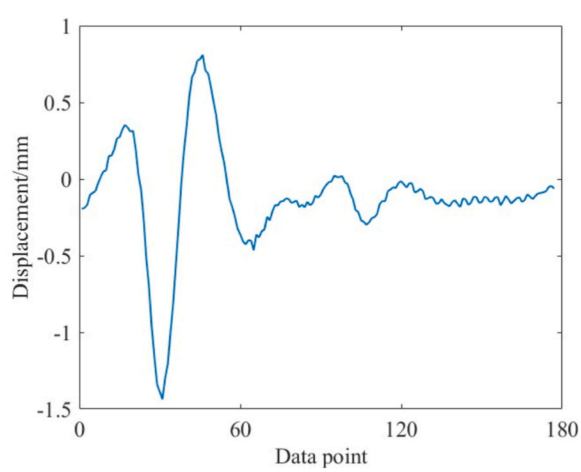

(b) sample of extracted data

Fig. 17. Preprocessing of measured data.

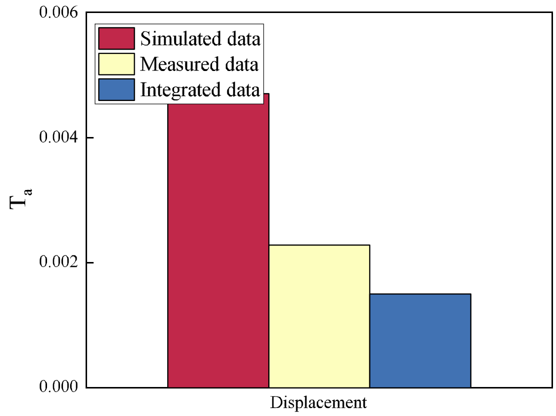

(a) T_a before and after data fusion

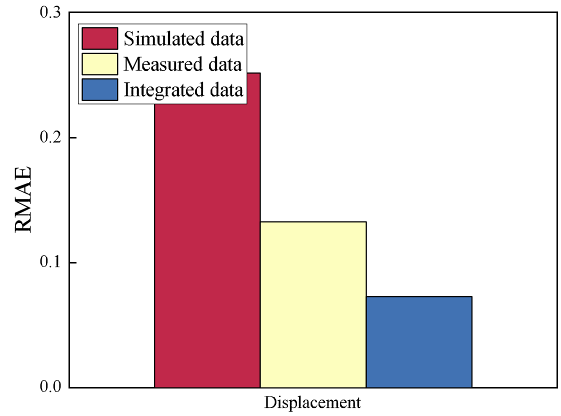

(b) *RMAE* before and after data fusion

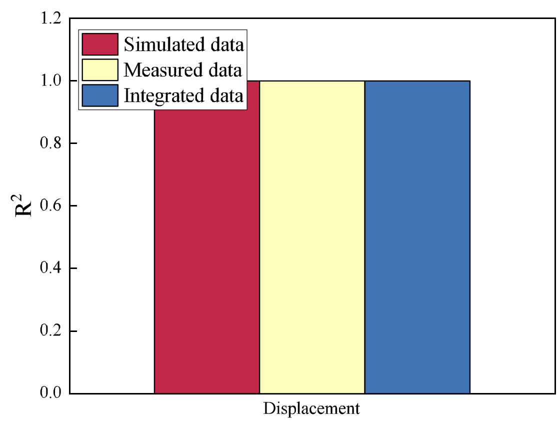

(c) R^2 before and after data fusion

Fig. 18. Comparison of evaluation metrics before and after incorporating measured data.

3.1. Vehicle loads and numerical model

3.1.1. Vehicle classification

As advancements in vehicle manufacturing technology and evolving market demands lead to increased diversity in vehicle design dimensions and forms, it becomes impractical to analyze and calculate the impact of each individual vehicle on a bridge due to the enormous volume of traffic. Therefore, it is essential to focus on the commonalities among different vehicles and to extract representative vehicle models for analysis.

The vehicle load data utilized in this study were collected from the weigh-in-motion system installed at bridge A over a five-month period from May to September 2021. This dataset encompasses various vehicle load parameters, including monitoring time, lane, vehicle type, velocity, weight, number of axles, and axle weight. Analyzing the information from over six million vehicles recorded during this period, vehicle types were categorized into five distinct models: two-axle, three-axle, four-axle, five-axle, and six-axle vehicles. The detailed axle spacing parameters for these vehicle models are illustrated in Fig. 3. Given that the impact of vehicle weight on the bridge is primarily reflected through the influence of each axle's weight, the axle weight distribution was subsequently determined following the establishment of axle spacing for each vehicle model, as presented in Table 1.

3.1.2. Statistical analysis of vehicle weight and velocity

Statistical analysis was conducted on vehicle weight and velocity data using probability and mathematical statistics methods to establish the probability distribution model of vehicle loads, thereby providing a theoretical foundation for subsequent vehicle load data simulation. Gaussian Mixture Models were applied to fit the vehicle weight and velocity data, with the fitting validated using the K-S test at a significance level of 0.05. Taking two-axle and five-axle vehicles as examples, the fitting curves for vehicle weight and velocity are depicted in Fig. 4 and Fig. 5, respectively. The calculations reveal that the average vehicle weight for two-axle vehicles is 2.89 t, with an average velocity of 97.55 km/h; for three-axle vehicles, the average weight is 17.89 t, and the average velocity is 79.67 km/h; for four-axle vehicles, the average weight is 25.13 t, and the average velocity is 79.52 km/h; for five-axle vehicles, the average weight is 29.09 t, and the average velocity is 77.02 km/h; and for six-axle vehicles, the average weight is 40.03 t, and the average velocity is 77.49 km/h. Compared to other vehicle types, two-axle vehicles exhibit a significantly lower average weight but a much higher average velocity. This discrepancy is primarily due to the fact that most two-axle vehicles consist of sedans and sport utility vehicles, which are generally lighter and faster.

While generating samples directly from the probability distribution fitted by the GMM is straightforward and easy to implement, traditional methods usually do not guarantee that the generated samples will strictly conform to the actual distribution. They may produce results that deviate from the reality, particularly in cases where the sample distribution is complex, as random generation may fail to effectively cover the entire sample space. In contrast, Markov Chain Monte Carlo (MCMC) sampling can generate samples from complex probability distributions, ensuring that the samples align with the true distribution.

Taking two-axle and five-axle vehicles as examples, the comparisons between the original data and the sampled data for vehicle weight and velocity are shown in Fig. 6 and Fig. 7. It can be observed that the probability density distribution histograms of the original data and the

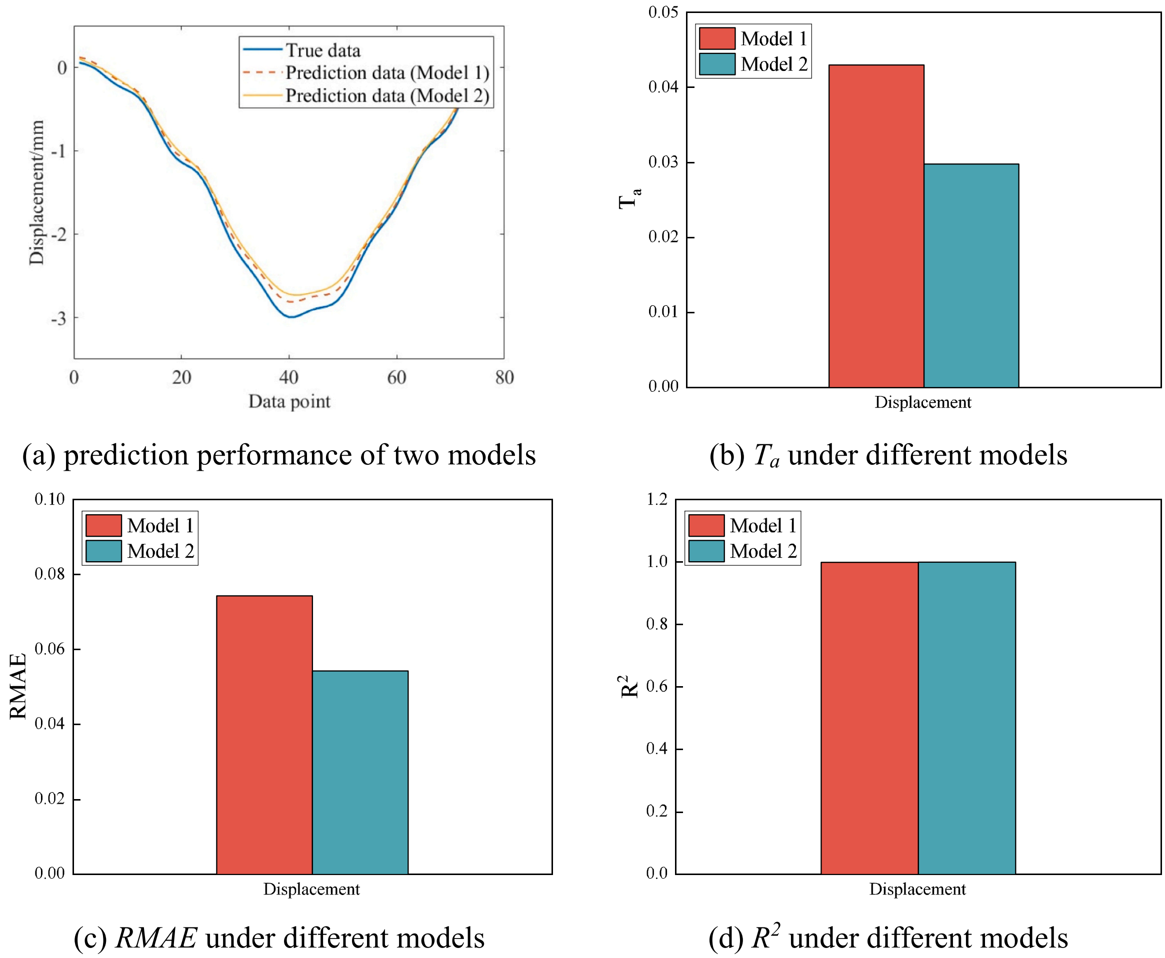

(a) prediction performance of two models

(b) T_a under different models

(c) *RMAE* under different models

(d) R^2 under different models

Fig. 19. Prediction results of the two models.

sampled data exhibit a high degree of similarity, indicating that the data samples obtained through the MCMC sampling method conform to the distribution characteristics of the original vehicle data.

3.1.3. Loading

Bridge A is modeled as a three-span continuous box girder with spans of 25 + 25 + 25 m. It consists of five small box girders and diaphragms, with a deck width of 17.3 m and beam height of 1.4 m. In fact, bridge A is a dual-span bridge in reality. This study aims to validate the feasibility of the digital twin framework for regional bridge groups. A single-span model is sufficient for this purpose while significantly reducing computational complexity. Therefore, the modeling and analysis of bridge A are based on a single-span scenario. The cross-sectional structure is depicted in Fig. 8. Bridge B and bridge C exhibit similar cross-sectional to bridge A, both comprising five small box girders and diaphragms. Bridge B is modeled as a single-span box girder with a span of 25 m, a deck width of 17 m, and beam height of 1.4 m. Bridge C is modeled as a single-span box girder with a span of 30 m, a deck width of 19 m, and beam height of 1.6 m. The similar cross-sectional structures of the three bridges facilitate the establish of the load response prediction model for these bridges. The loaded finite element model for bridge B is shown in Fig. 9.

The model was conducted using solid elements. After model updating, the concrete material parameters of bridge A were set as follows: elastic modulus of 34.5 GPa, Poisson's ratio of 0.18, and density of 2590 kg/m^3 . For bridge B and bridge C, which did not undergo load testing, the parameter settings were based on design specifications. The concrete material parameters for bridge B were set as: elastic modulus of 32 GPa, Poisson's ratio of 0.2, and density of 2530 kg/m^3 . For bridge C, the concrete material parameters were set as: elastic modulus of 35.5 GPa, Poisson's ratio of 0.2, and density of 2620 kg/m^3 .

Considering that a large amount of vehicle load data of transient dynamic analyses and complex computational of the finite element model of solid elements in this study, the mesh division must be optimized to balance computational accuracy with efficiency. After serval trial calculations, the mesh size was determined to be 0.5 m. Consequently, a single calculation for the continuous three-span model of bridge A takes approximately 15 minutes, while single calculations for the single-span models of bridge B and bridge C take about 5 minutes each.

In this study, vehicle load simulation data is applied to the finite element models to simulate the effects of vehicle loads on various bridges in real engineering conditions. When the distribution of vehicle load data reflects the actual proportions of different vehicle types in each lane, it is observed that the number of two-axle vehicles significantly exceeds that of other vehicle types, resulting in a disproportionately low representation of other vehicle types in the numerical simulation. This imbalance is not conducive to investigating the load effects of different vehicle types. Therefore, an equal number of five vehicle types were loaded onto different lanes during the actual loading process, with each type consisting of 100 vehicles, totaling 500 vehicles per lane.

The finite element models of the three bridges each include four lanes: the overtaking lane, the middle lane, the slow lane, and the emergency lane. Given that the emergency lane rarely experiences vehicle traffic, it was excluded from the analysis. Consequently, the

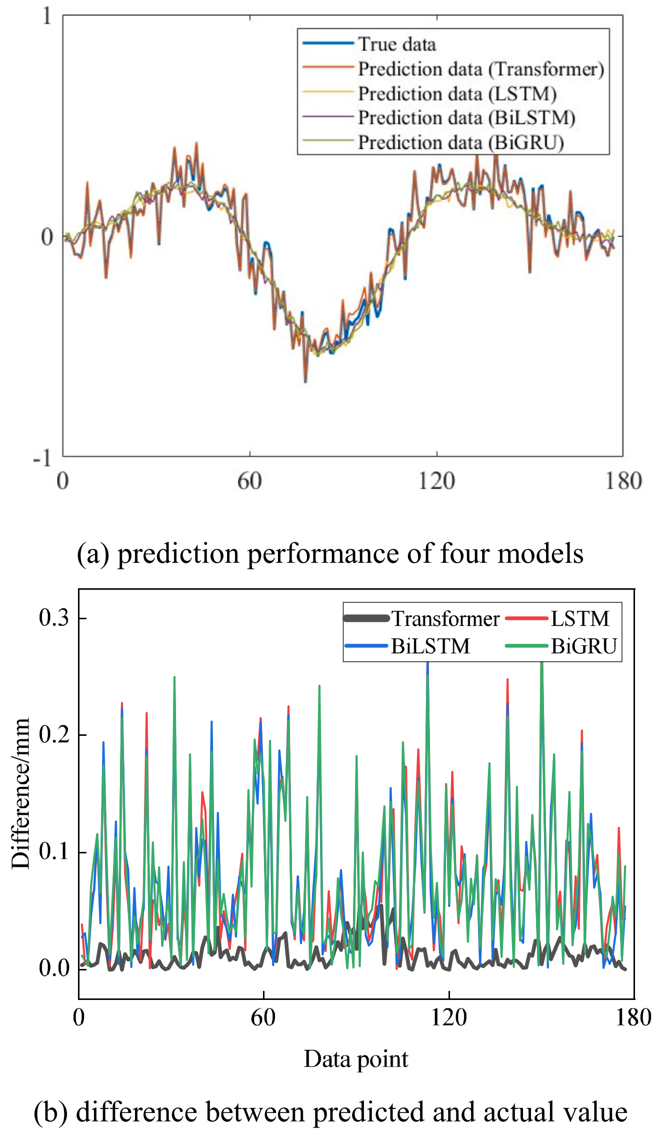

Fig. 20. Prediction performance of scenario 1.

loading was performed only on the overtaking lane, middle lane, and slow lane, leading to a total of 1500 vehicles being applied for each bridge. The vehicle loads include 16 parameters, namely: number of axles, lane, vehicle velocity, vehicle weight, and the weights of axles 1 through 6, vehicle length, wheelbase l_{12}, wheelbase l_{23}, wheelbase l_{34}, wheelbase l_{45}, and wheelbase l_{56}. Some vehicle load loading cases are shown in Table 2.

The application of 1500 sets of vehicle loads to the finite element models yielded the corresponding displacement responses of the bridges. To investigate the spatiotemporal relationships among various measurement points on the bridges, multiple measurement points were selected on the finite element models, with each point located at the bottom of a small box girder. For bridge A, 7 measurement points were arranged, with 5 points in the middle span and 2 points on each of the side spans, as shown in Fig. 10(a). Moreover, since bridge B and bridge C are both single-span box girder bridges, a similar arrangement was adopted, each with 5 measurement points, as illustrated in Fig. 10(b).

Taking a six-axle vehicle as an example, it was applied in the finite element analysis of three bridges, positioned in lane 2. The vehicle velocity is 88.77 km/h, and weight is 42.63 tons, with axle weights of 5.97 t, 5.97 t, 7.67 t, 7.67 t, 7.67 t, and 7.67 t. The vehicle length is 12.8 m, and the wheelbase are 3.2 m, 1.4 m, 5.4 m, 1.4 m, and 1.4 m.

Fig. 11 (a) and Fig. 11 (b) display the response of displacement in the middle and side spans of bridge A, respectively. Fig. 11 (c) and Fig. 11 (d) depict the displacement at measurement point 3 of bridges B and C, respectively. From the figures, it can be observed that bridge C exhibits a greater displacement amplitude compared to bridge B due to its greater span.

3.2. Response prediction based on loads

The generated 1500 sets of vehicle load data were sequentially applied to the finite element models of the three bridges, yielding 1500 corresponding sets of displacement response data for each bridge. For bridge A, each set of displacement response data include seven measurement points, whereas bridges B and C, each set includes five measurement points. Additionally, due to the variability in vehicle lengths, the time steps in each set of response data within a single bridge are different. To standardize the sequence lengths, zero-padding was employed at the end of the displacement response data sequences, ensuring that the length of each response data sequence matched the maximum sequence length of the bridge's response data. This zero-padding allows for uniform sequence lengths within each bridge's response data, thereby facilitating the development of the subsequent neural network prediction model.

Given the computational intensity of numerical simulations, the dataset was limited to 1500 sets, resulting in a relatively small data scale. To address this limitation, data augmentation techniques are usually utilized to generate time series data for deep learning networks. Among these techniques, the addition of noise, a prevalent method for enhancing time series data, is employed to increase the dataset size and mitigate the issue of insufficient data. It is important to note that the noise follows a Gaussian distribution with a mean of 0 and a small variance of 0.001, ensuring that the noise minimally impact the intrinsic characteristics of the original data. The comparison of data before and after adding noise is illustrated in Fig. 12.Through multiple experimentation, it was found that adding 3500 sets of data with noise, namely a total of 4500 data sets, produced satisfactory results for constructing the neural network prediction model. The prediction accuracy was not significantly improved by adding further data.

The displacement responses at measurement point 3 in the central span of bridge A, measurement point 6 in the side span of bridge A, measurement point 3 of bridge B, and measurement point 3 of bridge C were selected for the establishment of predictive models using the Transformer neural network. The vehicle load data was used to predict the displacement responses. The neural network models were trained, validated, and tested on the same dataset for all three bridges, with a total of 400 training epochs. The prediction results for the displacement responses at measurement points 3 of bridge A, as well as measurement point 3 of bridge B are illustrated as examples in Fig. 13 and Fig. 14. From the magnified sections, it can be observed that the model demonstrates a satisfactory fit. The regions with more pronounced variations are attributed to the noise added to the original data.

The prediction results of the displacement responses for all three bridges are summarized in Table 3. The smaller T_a and *RMAE* value indicate superior predictive performance of the model, while a larger R^2 value signifies that the predicted results closely approximate the actual values. The prediction accuracy for the side span of bridge A is the highest due to its relatively simple displacement response. It is notable that the R^2 values for all four measurement points exceed 0.99, demonstrating that the results are sufficiently accurate to meet engineering requirements. Within the digital twin system of the bridges group, the responses of the bridges can be readily computed through the pre-trained models, thereby obviating the necessity for extensive calculations using finite element models.

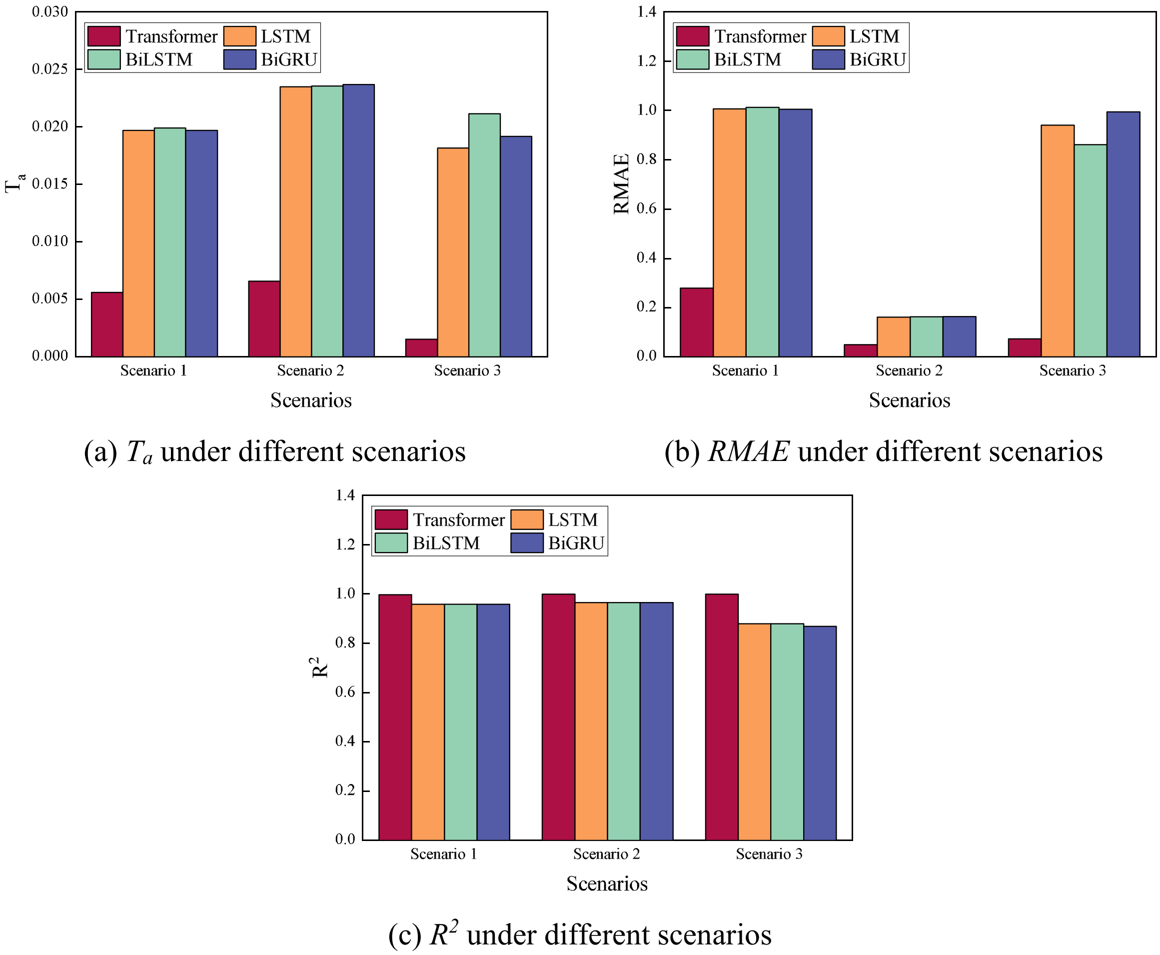

(a) T_a under different scenarios

(b) *RMAE* under different scenarios

(c) R^2 under different scenarios

Fig. 21. Evaluation metrics under different scenarios.

Table 4
The value of T_a under different scenarios.

Network	Scenario 1	Scenario 2	Scenario 3
Transformer	0.0056	0.0066	0.0015
LSTM	0.0197	0.0235	0.0182
BiLSTM	0.0199	0.0236	0.0211
BiGRU	0.0197	0.0237	0.0192

Table 5
The value of *RMAE* under different scenarios.

Network	Scenario 1	Scenario 2	Scenario 3
Transformer	0.2795	0.0499	0.0730
LSTM	1.0064	0.1614	0.9407
BiLSTM	1.0128	0.1621	0.8611
BiGRU	1.0050	0.1635	0.9949

Table 6
The value of R^2 under different scenarios.

Network	Scenario 1	Scenario 2	Scenario 3
Transformer	0.9970	0.9998	0.9992
LSTM	0.9581	0.9657	0.880
BiLSTM	0.9576	0.9656	0.8793
BiGRU	0.9582	0.9651	0.8686

3.3. Bridge response prediction based on response

The previous section discussed the prediction model of displacement responses based on vehicle load. The following section investigates the situation of WIM system failure within the digital twin system of the bridges group, resulting in the unavailability of timely vehicle information. Consequently, the model for mutual prediction of displacement responses at different measurement points between bridges is undertaken to ensure the normal operation of the digital twin system. Generally, each bridge was equipped with multiple displacement measurement points, one measurement point can be used to predict another point, or several points can be used to predict the response at a single point. Although a many-to-one model can integrate information from multiple measurement points, providing a more comprehensive data prediction and capturing the overall dynamics more effectively, a one-to-one model offers a more focus on the relationship between individual measurement points. This latter approach yields a simpler, more easily implemented prediction model. Moreover, the accuracy achieved by the model is deemed sufficiently satisfactory. Therefore, the one-to-one model was established to achieve the prediction of the response.

Four one-to-one response prediction models were constructed to explore the influence of different bridges on the prediction of measurement point responses. These models are as follows:

1) predicting the response at point 3 of bridge A using data from point 1 of bridge A;
2) predicting the response at point 3 of bridge B using data from point 3 of bridge A;

3) predicting the response at point 3 of bridge C using data from point 3 of bridge A;
4) predicting the response at point 3 of bridge C using data from point 3 of bridge B.

Fig. 15 illustrates the predictive performance of the four models across different evaluation metrics. From Fig. 15 (a) and (b), it can be observed that the accuracy of models 2–4 progressively improves. Notably, in models 2 and 3, the responses of single-span bridges B and C are predicted using data from the three-span bridge A, leading to lower accuracy due to the significant differences between the bridges. Conversely, model 4, which predicts between two single-span bridges, demonstrates slightly higher accuracy. Additionally, considering that bridge C has a longer span and larger displacement values compared to bridge B, its greater resistance to noise enhances the predictive performance of model 3 over model 2. At last, although model 1 focuses on predictions between two measurement points within bridge A, its predictive accuracy is relatively modest, suggesting that the relationship of measurement points between middle spans of different bridges is more easily learned. As shown in Fig. 15 (c), the coefficient of determination R^2 for all four models exhibits minimal differences and is nearly equal to 1, indicating excellent model fits that meet the requirements for engineering applications.

4. Experimental validation

4.1. Data fusion

Bridge A is equipped with the structure health monitoring system, making it feasible to integrate both measured and simulated data for predicting the bridge's response. The bridge A, as well as the dynamic displacement sensors installed, are illustrated in Fig. 16. Fig. 16(b) is a dual-span bridge, while all analyses and models in this study are based on a single-span bridge. Fig. 16(d) displays the sensor layout at the midspan cross-section of the bridge, with all measurement points arranged at the bottom of the box girder.

Due to the high sampling frequency of 200 Hz from the dynamic displacement sensors, which significantly exceeds that of the simulated data and causes huge computing burden for the system, a downsampling procedure was employed to facilitate the integration of measured and simulated data. After multiple trials, it was determined that extracting one effective data point every ten data points, thereby reducing the sampling frequency from 200 Hz to 20 Hz, yielded the most effective results. The resulting data sequences were then segmented according to a preset length. Subsequently, 4500 data sets were randomly selected and integrated with the simulated data for the prediction of bridge responses. Fig. 17 shows the preprocessing of the measured data.

After mixing 4500 sets of measured data with 4500 sets of simulated data, 9000 sets of displacement data were obtained. Then the combined datasets were shuffled and input into the Transformer model for training and prediction. This is analogous to Case 1 discussed in the preceding section, predicting the displacement at point 3 of bridge A using data from point 1 of bridge A. Fig. 18 presents a comparison of the evaluation metrics for the prediction results using the simulated data alone versus the mixed dataset. The results indicate a significant reduction in both the T_a and *RMAE* metrics, accompanied by a slight fluctuation in R^2. T_a and *RMAE* suggest a marked enhancement in the predictive performance, demonstrating that the integration of measured data contributes to increasing accuracy in response prediction.

4.2. Model application

A vehicle was driven at the same velocity successively over bridge A and bridge B, with sensors temporarily installed on bridge B to validate the pre-trained response prediction models. Model 1 involves predicting the displacement response of point 3 at the midspan of bridge B based on vehicle load, while Model 2 predicts the displacement of point 3 of bridge B using data from point 3 of bridge A. The performance of the digital twin system for the bridges group is evaluated by comparing the predicted responses from the two models with the actual responses measured by the sensors. Fig. 19 displays the prediction results. As shown in Fig. 19 (a), both models achieve good results, predict dynamic displacement close to the true values. Obviously, the prediction performance of Model 2 is superior to that of Model 1, as the response provides more comprehensive information than the vehicle load. However, the prediction accuracy of Model 1 is also sufficient for practical engineering applications.

5. Discussion

To better understand the capabilities of the Transformer model, displacement response predictions were also conducted using LSTM, Bi-directional Long Short-Term Memory (BiLSTM), and Bi-directional Gated Recurrent Unit (BiGRU) models under identical conditions. Three distinct scenarios were evaluated, given as flows:

Scenario 1: Predicting the displacement response of point 3 at the midspan of bridge A based on vehicle load;
Scenario 2: Predicting the displacement of point 3 at the midspan of bridge B using the displacement data from point 3 of bridge A;
Scenario 3: Integrating measured and simulated data to predict the displacement of point 3 at the midspan of bridge A using displacement data at point 1.

Taking Scenario 1 as an example, a segment of displacement response was extracted, and the prediction performance is shown in Fig. 20 (a), which illustrates the prediction performance of the Transformer, LSTM, BiLSTM, and BiGRU models. It is evident from the figure that the prediction accuracy of other models is quite similar, capturing only the general trend of the response. In contrast, the Transformer model demonstrates superior performance, accurately predicting the displacement response with only slight discrepancies in certain areas. Furthermore, the absolute value of the difference between predicted value and actual value is shown in Fig. 20 (b), which more clearly demonstrates the accuracy of the Transformer model.

The evaluation metrics across the three scenarios are depicted in Fig. 21. It can be observed that the Transformer model significantly outperforms the other three models, with much lower T_a and *RMAE* values across all scenarios, and R^2 values that are closer to 1, indicating the superior predictive accuracy of the Transformer model. The performance of the other three models is nearly identical in scenarios 1 and 2, whereas their evaluation metrics exhibit a larger variance in scenario 3. This difference in scenario 3 is likely due to the doubled data volume and the increased complexity in response prediction arising from the integration of measured and simulated data. The specific values of each indicator in the figures are listed in Tables 4, 5, and 6. Furthermore, additional comparative analyses in similar scenarios, such as predicting bridge B's response from vehicle load data or predicting bridge C's response based on bridge A's response, revealed consistent trends. Due to space constraints, these findings are not elaborated here.

Despite the promising results, this study has several limitations that warrant further investigation. Firstly, the numerical simulations assume vehicles passing the bridge individually, which simplifies real-world traffic dynamics such as vehicle queues and congestion. Future work will incorporate more realistic traffic flow models and explore advanced data augmentation techniques (e.g., Generative Adversarial Networks) to better capture spatiotemporal dependencies. Secondly, the computational cost of training multiple Transformer models for bridges with numerous measurement points could hinder real-time applications. Transfer learning strategies will be investigated to enhance efficiency. Thirdly, the accuracy of the digital twin framework relies heavily on the finite element models of the bridges. To ensure long-term reliability, regular load tests will be conducted on the three bridges to update the model parameters and maintain prediction accuracy. Lastly, while the current framework is validated on box girder bridges, its generalizability to other bridge types (e.g., arch bridges, cable-stayed bridges) remains to be explored. Addressing these challenges will advance the digital twin's adaptability to complex traffic scenarios and diverse infrastructure systems, ultimately supporting intelligent management of regional bridge networks.

6. Conclusion

This study introduces a digital twin system for regional bridges group, specifically designed to mitigate the challenges posed by the lack of health monitoring systems on many bridges and to improve the intelligent operation and maintenance of regional bridge networks. In the bridges group, the response prediction model is constructed using a Transformer network and three scenarios are investigated: predicts bridge responses based on vehicle loads, predicts bridge responses both within a single bridge and across different bridges, and predicts responses with the fusion of measured data. Scenario 1 represents the most prevalent application, facilitating the prediction of bridge responses upon obtaining vehicle information. Scenario 2 enables the prediction of responses for other bridges within the group, even after a failure of the WIM system, by utilizing sensors installed on specific bridges. Scenario 3 effectively integrates mitigates potential deficiencies in the monitoring data. These scenarios demonstrate the significant advantages of the digital twin system and its resilience against adverse interferences, thereby supporting the implementation of management and maintenance decision-making for the bridges network.

At last, a vehicle was driven over bridges to validate the pre-trained response prediction models within the network. The accuracy and robustness of the predictions are evaluated using three performance metrics: T_a, *RMAE*, and R^2. Furthermore, the predictive efficacy of the Transformer model is compared with that of LSTM, BiLSTM, and BiGRU models across the same scenarios.

The main conclusions are as follows:

1. Response prediction based on vehicle loads: The prediction of the side span response using vehicle load data demonstrated the highest performance among all cases. This can be attributed to the relative simplicity of the time-displacement curve associated with the side span.
2. Response prediction between bridges: The prediction of bridge responses was most accurate when the structural characteristics of the bridges were closely aligned, highlighting the influence of structural similarity on predictive performance.
3. Integration of measured and simulated data: The fusion of measured data with simulated data markedly enhanced the model's predictive accuracy, underscoring the significant role of data integration in improving the precision and reliability of prediction outcomes.
4. Model validation: Although the accuracy of the neural network trained on simulated data decreases during actual validation, it continues to satisfy the practical requirements of engineering applications.

The digital twin system developed in this study effectively utilizes regional vehicle information and monitoring information from bridges equipped with health monitoring systems. This model holds particular promise for bridges that lack such monitoring capabilities, thereby enhancing the intelligent management and maintenance of the broader regional bridge network. The proposed methodology demonstrates significant potential for long-term health monitoring applications of actual bridge groups, particularly beam bridges. Future research will focus on conducting load tests on bridges without monitoring systems to develop more accurate finite element models, and will explore the interrelationships of response predictions among various bridge types within the bridge network to facilitate intelligent management and maintenance strategies.

CRediT authorship contribution statement

Peng Haoyan: Visualization. **Xue Songtao:** Writing – review & editing. **Zhang Guangcai:** Validation, Software. **Ding Youliang:** Methodology. **Xie Liyu:** Visualization. **Zhao Wenlong:** Writing – original draft, Software, Investigation, Data curation. **Wan Chunfeng:** Writing – review & editing, Funding acquisition. **Zhang Xiaonan:** Data curation.

Declaration of Competing Interest

The authors declare that they have no known competing financial interests or personal relationships that could have appeared to influence the work reported in this paper.

Acknowledgments

The authors acknowledge the financial support provided by National Natural Science Foundation of China (52178119) and Research Fund for Advanced Ocean Institute of Southeast University, Nantong (GP202409).

Appendix A. Supporting information

Supplementary data associated with this article can be found in the online version at doi:10.1016/j.istruc.2025.109052.

References

[1] Qi Q, Tao F, Hu T, Anwer N, Liu A, Wei Y, et al. Enabling technologies and tools for digital twin. J Manuf Syst 2021;58:3–21. https://doi.org/10.1016/j.jmsy.2019.10.001.
[2] Lu Y, Liu C, Wang KI-K, Huang H, Xu X. Digital Twin-driven smart manufacturing: connotation, reference model, applications and research issues. Robot Comput-Integr Manuf 2020;61:101837. https://doi.org/10.1016/j.rcim.2019.101837.
[3] Tao F, Xiao B, Qi Q, Cheng J, Ji P. Digital twin modeling. J Manuf Syst 2022;64:372–89. https://doi.org/10.1016/j.jmsy.2022.06.015.
[4] Schluse M, Priggemeyer M, Atorf L, Rossmann J. Experimentable digital twins-streamlining simulation-based systems engineering for industry 4.0. IEEE Trans Ind Inf 2018;14:1722–31. https://doi.org/10.1109/TII.2018.2804917.
[5] Liu Q, Zhang H, Leng J, Chen X. Digital twin-driven rapid individualised designing of automated flow-shop manufacturing system. Int J Prod Res 2019;57:3903–19. https://doi.org/10.1080/00207543.2018.1471243.
[6] Tao F, Cheng J, Qi Q, Zhang M, Zhang H, Sui F. Digital twin-driven product design, manufacturing and service with big data. Int J Adv Manuf Technol 2018;94:3563–76. https://doi.org/10.1007/s00170-017-0233-1.
[7] Qi Q, Tao F. Digital twin and big data towards smart manufacturing and industry 4.0: 360 degree comparison. IEEE Access 2018;6:3585–93. https://doi.org/10.1109/ACCESS.2018.2793265.
[8] Broo DG, Schooling J. Digital twins in infrastructure: definitions, current practices, challenges and strategies. Int J Constr Manag 2023;23:1254–63. https://doi.org/10.1080/15623599.2021.1966980.
[9] Pregnolato M, Gunner S, Voyagaki E, De Risi R, Carhart N, Gavriel G, et al. Towards Civil Engineering 4.0: Concept, workflow and application of Digital Twins for existing infrastructure. Autom Constr 2022;141:104421. https://doi.org/10.1016/j.autcon.2022.104421.
[10] Zhang X, Ding Y, Zhao H, Yi L, Guo T, Li A, et al. Mixed skewness probability modeling and extreme value predicting for physical system input-output based on full Bayesian generalized maximum-likelihood estimation. IEEE Trans Instrum Meas 2024;73:2504516. https://doi.org/10.1109/TIM.2023.3343742.
[11] Webb GT, Vardanega PJ, Middleton CR. Categories of SHM deployments: technologies and capabilities. J Bridge Eng 2015;20:04014118. https://doi.org/10.1061/(ASCE)BE.1943-5592.0000735.
[12] Wang W, Dan D, Gao J. Study on damage identification of High-Speed railway truss bridge based on statistical steady-state strain characteristic function. Eng Struct 2023;294:116723. https://doi.org/10.1016/j.engstruct.2023.116723.
[13] Wei Y-T, Yi T-H, Yang D-H, Liu H, Deng Y. Unsupervised stiffness evaluation of high-speed railway bridges using periodic monitoring data. J Bridge Eng 2024;29:04024002. https://doi.org/10.1061/JBENF2.BEENG-6561.
[14] Dan D, Ying Y, Ge L. Digital twin system of bridges group based on machine vision fusion monitoring of bridge traffic load. IEEE Trans Intell Transp Syst 2022;23:22190–205. https://doi.org/10.1109/TITS.2021.3130025.

[15] Dang N, Shim C. Bridge assessment for PSC girder bridge using digital twins model, 54. Springer Science and Business Media Deutschland GmbH; 2020. p. 1241–6. https://doi.org/10.1007/978-981-15-0802-8_199.
[16] Bittencourt TN, Futai MM, da Conceicao Neto AP, Ribeiro DM. Digital transformation of bridges inspection, monitoring and maintenance processes. In: Yokota H, Frangopol DM, editors. Bridge maintenance, safety, management, life-cycle sustainability and innovations. Leiden: CRC Press-Balkema; 2021. p. 11–30. https://doi.org/10.1201/9780429279119-2.
[17] Saback V, Popescu C, Blanksvard T, Taljsten B. Asset management of existing concrete bridges using digital twins and BIM: a state-of-the-art literature review. Nord Concr Res 2022;66:91–111. https://doi.org/10.2478/ncr-2021-0020.
[18] Kaewunruen S, AbdelHadi M, Kongpuang M, Pansuk W, Remennikov AM. Digital twins for managing railway bridge maintenance, resilience, and climate change adaptation. Sensors 2023;23:252. https://doi.org/10.3390/s23010252.
[19] Zhang G, Wan C, Xie L, Xue S. Structural damage identification with output-only measurements using modified Jaya algorithm and Tikhonov regularization method. Smart Struct Syst 2023;31:229–45. https://doi.org/10.12989/sss.2023.31.3.229.
[20] Zhang G, Kang J, Wan C, Xie L, Xue S. Output-only structural damage identification based on Q-learning hybrid evolutionary algorithm and response reconstruction technique. Measurement 2024;224:113951. https://doi.org/10.1016/j.measurement.2023.113951.
[21] Xu Z-D, Li S, Zeng X. Distributed strain damage identification technique for long-span bridges under ambient excitation. Int J Struct Stab Dyn 2018;18:1850133. https://doi.org/10.1142/S021945541850133X.
[22] Ye C, Butler L, Calka B, Iangurazov M, Lu Q, Gregory A, et al. A digital twin of bridges for structural health monitoring. DEStech Publications, Inc; 2019. https://doi.org/10.17863/CAM.63903.
[23] Jiang F, Ding Y, Song Y, Geng F, Wang Z. An architecture of lifecycle fatigue management of steel bridges driven by Digital Twin. Struct Monit Maint 2021;8:187–201. https://doi.org/10.12989/smm.2021.8.2.187.
[24] Jiang F, Ding Y, Song Y, Geng F, Wang Z. Digital Twin-driven framework for fatigue life prediction of steel bridges using a probabilistic multiscale model: application to segmental orthotropic steel deck specimen. Eng Struct 2021;241:112461. https://doi.org/10.1016/j.engstruct.2021.112461.
[25] Kang J-S, Chung K, Hong EJ. Multimedia knowledge-based bridge health monitoring using digital twin. Multimed Tools Appl 2021;80:34609–24. https://doi.org/10.1007/s11042-021-10649-x.
[26] Dang H, Tatipamula M, Nguyen HX. Cloud-based digital twinning for structural health monitoring using deep learning. IEEE Trans Ind Inf 2022;18:3820–30. https://doi.org/10.1109/TII.2021.3115119.
[27] Zhao H, Tan C, OBrien EJ, Zhang B, Uddin N, Guo H. Developing digital twins to characterize bridge behavior using measurements taken under random traffic. J Bridge Eng 2022;27:04021101. https://doi.org/10.1061/(ASCE)BE.1943-5592.0001814.
[28] Zanelli F, Debattisti N, Mauri M, Argentino A, Belloli M. Development and field validation of wireless sensors for railway bridge modal identification. Appl Sci-Basel 2023;13:3620. https://doi.org/10.3390/app13063620.
[29] Zhao H, Ding Y, Li A, Chen B, Zhang X. State-monitoring for abnormal vibration of bridge cables focusing on non-stationary responses: From knowledge in phenomena to digital indicators. Measurement 2022;205:112148. https://doi.org/10.1016/j.measurement.2022.112148.
[30] Zhao H, Ding Y, Meng L, Qin Z, Yang F, Li A. Bayesian multiple linear regression and new modeling paradigm for structural deflection robust to data time lag and abnormal signal. IEEE Sens J 2023;23:19635–47. https://doi.org/10.1109/JSEN.2023.3294912.
[31] Xu Z-D, Liu M, Wu Z, Zeng X. Energy damage detection strategy based on strain responses for long-span bridge structures. J Bridge Eng 2011;16:644–52. https://doi.org/10.1061/(ASCE)BE.1943-5592.0000195.
[32] Xu Z-D, Zeng X, Li S. Damage detection strategy using strain-mode residual trends for long-span bridges. J Comput Civ Eng 2015;29:04014064. https://doi.org/10.1061/(ASCE)CP.1943-5487.0000371.
[33] Xia Y, Jian X, Yan B, Su D. Infrastructure safety oriented traffic load monitoring using multi-sensor and single camera for short and medium span bridges. Remote Sens 2019;11:2651. https://doi.org/10.3390/rs11222651.
[34] Kuddus MA, Li J, Hao H, Li C, Bi K. Target-free vision-based technique for vibration measurements of structures subjected to out-of-plane movements. Eng Struct 2019;190:210–22. https://doi.org/10.1016/j.engstruct.2019.04.019.
[35] Jian X, Xia Y, Lozano-Galant JA, Sun L. Traffic sensing methodology combining influence line theory and computer vision techniques for girder bridges. J Sens 2019;2019:3409525. https://doi.org/10.1155/2019/3409525.
[36] Xue X, Zhu H, Chen Y, Wang Y. Research on Construction of Digital Twin System for Bridge Vehicle Load Identification. 2022 8TH INternational Conference On Hydraulic And Civil Engineering: Deep Space Intelligent Development And Utilization Forum, ICHCE. New York: IEEE; 2022. p. 536–9. https://doi.org/10.1109/ICHCE57331.2022.10042557.
[37] Hou R, Jeong S, Lynch JP, Law KH. Cyber-physical system architecture for automating the mapping of truck loads to bridge behavior using computer vision in connected highway corridors. Transp Res Pt C-Emerg Technol 2020;111:547–71. https://doi.org/10.1016/j.trc.2019.11.024.
[38] Yu S, Li D, Ou J. Digital twin-based structure health hybrid monitoring and fatigue evaluation of orthotropic steel deck in cable-stayed bridge. Struct Control Health Monit 2022;29:e2976. https://doi.org/10.1002/stc.2976.
[39] Tang J, Heng J, Feng L, Yu Z, Zhou Z, Baniotopoulos C. Digital twins-boosted identification of bridge vehicle loads integrating video and physics. Comput Struct 2024;305:107578. https://doi.org/10.1016/j.compstruc.2024.107578.
[40] An P, Wang Z, Zhang C. Ensemble unsupervised autoencoders and Gaussian mixture model for cyberattack detection. Inf Process Manag 2022;59:102844. https://doi.org/10.1016/j.ipm.2021.102844.
[41] Dou H, Liu Y, Chen S, Zhao H, Bilal H. A hybrid CEEMD-GMM scheme for enhancing the detection of traffic flow on highways. Soft Comput 2023;27:16373–88. https://doi.org/10.1007/s00500-023-09164-y.
[42] Zhou J, Qin Y, Luo J, Zhu T. Remaining useful life prediction by distribution contact ratio health indicator and consolidated memory GRU. IEEE Trans Ind Inf 2023;19:8472–83. https://doi.org/10.1109/TII.2022.3218665.
[43] Ma X, Tao Z, Wang Y, Yu H, Wang Y. Long short-term memory neural network for traffic speed prediction using remote microwave sensor data. Transp Res Pt C-Emerg Technol 2015;54:187–97. https://doi.org/10.1016/j.trc.2015.03.014.
[44] Chung J, Gulcehre C, Cho K, Bengio Y. Gated Feedback Recurrent Neural Networks. vol. 37. In: Bach F, Blei D, editors. INternational Conference On Machine Learning, 37. San Diego: Jmlr-Journal Machine Learning Research; 2015. p. 2067–75. vol. 37.
[45] Ding Y, Jia M, Miao Q, Cao Y. A novel time–frequency Transformer based on self–attention mechanism and its application in fault diagnosis of rolling bearings. Mech Syst Signal Process 2022;168:108616. https://doi.org/10.1016/j.ymssp.2021.108616.
[46] Flah M, Nunez I, Ben Chaabene W, Nehdi ML. Machine learning algorithms in civil structural health monitoring: a systematic review. Arch Comput Method Eng 2021;28:2621–43. https://doi.org/10.1007/s11831-020-09471-9.